

2018

**Insights into the magnetic dead layer in La<sub>0.7</sub>Sr<sub>0.3</sub>MnO<sub>3</sub> thin films from temperature, magnetic field and thickness dependence of their magnetization**

N. Mottaghi

M.S. Seehra


R. Trappen

S. Kumari

Chih-Yeh Huang

*See next page for additional authors*

Follow this and additional works at: [https://researchrepository.wvu.edu/faculty\\_publications](https://researchrepository.wvu.edu/faculty_publications)

 Part of the [Aerospace Engineering Commons](#), [Astrophysics and Astronomy Commons](#), [Mechanical Engineering Commons](#), and the [Physics Commons](#)

---

---

**Authors**

N. Mottaghi, M.S. Seehra, R. Trappen, S. Kumari, Chih-Yeh Huang, S. Yousefi, G.B. Cabrera, A.H. Romero, and M.B. Holcomb

---

# Insights into the magnetic dead layer in $\text{La}_{0.7}\text{Sr}_{0.3}\text{MnO}_3$ thin films from temperature, magnetic field and thickness dependence of their magnetization

Cite as: AIP Advances **8**, 056319 (2018); <https://doi.org/10.1063/1.5005913>

Submitted: 20 September 2017 . Accepted: 03 November 2017 . Published Online: 10 January 2018

N. Mottaghi, M. S. Seehra, R. Trappen, S. Kumari, Chih-Yeh Huang, S. Yousefi, G. B. Cabrera, A. H. Romero, and M. B. Holcomb

## COLLECTIONS

Paper published as part of the special topic on [62nd Annual Conference on Magnetism and Magnetic Materials](#)



View Online



Export Citation



CrossMark


## ARTICLES YOU MAY BE INTERESTED IN

[Tuning the dead-layer behavior of  \$\text{La}\_{0.67}\text{Sr}\_{0.33}\text{MnO}\_3/\text{SrTiO}\_3\$  via interfacial engineering](#)  
Applied Physics Letters **104**, 081606 (2014); <https://doi.org/10.1063/1.4866461>

[Strain-dependent magnetic phase diagram of epitaxial  \$\text{La}\_{0.67}\text{Sr}\_{0.33}\text{MnO}\_3\$  thin films](#)  
Applied Physics Letters **76**, 2421 (2000); <https://doi.org/10.1063/1.126363>

[The role of strain in magnetic anisotropy of manganite thin films](#)  
Applied Physics Letters **71**, 140 (1997); <https://doi.org/10.1063/1.119454>



NEW



## AVS Quantum Science

A new interdisciplinary home for impactful quantum science research and reviews

Co-Published by

NOW ONLINE



## Insights into the magnetic dead layer in $\text{La}_{0.7}\text{Sr}_{0.3}\text{MnO}_3$ thin films from temperature, magnetic field and thickness dependence of their magnetization

N. Mottaghi,<sup>1,a</sup> M. S. Seehra,<sup>1</sup> R. Trappen,<sup>1</sup> S. Kumari,<sup>1</sup> Chih-Yeh Huang,<sup>2</sup> S. Yousefi,<sup>1</sup> G. B. Cabrera,<sup>1</sup> A. H. Romero,<sup>1</sup> and M. B. Holcomb<sup>1</sup>

<sup>1</sup>Department of Physics & Astronomy, West Virginia University, Morgantown, WV 26506, USA

<sup>2</sup>Department of Mechanical & Aerospace Engineering, West Virginia University, Morgantown, WV 26506, USA

(Presented 10 November 2017; received 20 September 2017; accepted 3 November 2017; published online 10 January 2018)

Experimental investigations of the magnetic dead layer in 7.6 nm thick film of  $\text{La}_{0.7}\text{Sr}_{0.3}\text{MnO}_3$  (LSMO) are reported. The *dc* magnetization (*M*) measurements for a sample cooled to  $T = 5$  K in applied field  $H = 0$  reveal the presence of negative remanent magnetization (NRM) in the *M* vs. *H* (magnetic field) measurements as well as in the *M* vs. *T* measurements in  $H = 50$  Oe and 100 Oe. The *M* vs. *T* data in *ZFC* (zero-field-cooled) and *FC* (field-cooled) protocols are used to determine the blocking temperature  $T_B$  in different *H*. Isothermal hysteresis loops at different *T* are used to determine the temperature dependence of saturation magnetization ( $M_S$ ), remanence ( $M_R$ ) and coercivity  $H_C$ . The  $M_S$  vs. *T* data are fit to the Bloch law,  $M_S(T) = M_0(1 - BT^{-3/2})$ , showing a good fit for  $T < 100$  K and yielding the nearest-neighbor exchange constant  $J/k_B \cong 18$  K. The variations of  $T_B$  vs. *H* and  $H_C$  vs. *T* are well described by the model often used for randomly oriented magnetic nanoparticles with magnetic domain diameter  $\approx 9$  nm present in the dead-layer of thickness  $d = 1.4$  nm. Finally, the data available from literature on the thickness (*D*) variation of Curie temperature ( $T_C$ ) and  $M_S$  of LSMO films grown under 200, 150, and 0.38 mTorr pressures of  $\text{O}_2$  are analyzed in terms of the finite-size scaling, with  $M_S$  vs. *D* data fit to  $M_S(D) = M_S(b)(1-d/D)$  yielding the dead layer thickness  $d = 1.1$  nm, 1.4 nm and 2.4 nm respectively. Brief discussion on the significance of these results is presented. © 2018 Author(s). All article content, except where otherwise noted, is licensed under a Creative Commons Attribution (CC BY) license (<http://creativecommons.org/licenses/by/4.0/>). <https://doi.org/10.1063/1.5005913>

Mixed valence manganese oxides with the formula  $\text{RE}_{1-x}\text{A}_x\text{MnO}_3$  (RE = trivalent rare earth element; A = divalent alkaline earth element) have a wide range of electronic and magnetic phases depending on doping level and cation radii, making them useful in spintronic and magnetic memory devices.<sup>1</sup> Studies of thin films of  $\text{La}_{1-x}\text{A}_x\text{MnO}_3$  showed above room temperature Curie temperature  $T_C \sim 370$  K is achieved by doping Sr at the A-site with an optimum ratio of  $x \sim 0.3$ ,<sup>2</sup> making  $\text{La}_{0.7}\text{Sr}_{0.3}\text{MnO}_3$  thin films good candidates for resistive switching memory devices, ferroelectric/ferromagnetic systems and heterostructures.<sup>3-5</sup> Studies on thin films of  $\text{La}_{0.7}\text{Sr}_{0.3}\text{MnO}_3$  also showed that their magnetic properties are affected by film thickness and an inactive magnetic layer (dead layer) is present in thin films. Huijben *et al.* performed magnetic and transport measurements on LSMO thin films fabricated by pulsed laser deposition (PLD) with different thicknesses and reported that thin films remain ferromagnetic down to 3 unit cells.<sup>6</sup> Monsen *et al.* studied the thickness dependence of magnetic properties of LSMO thin films and determined a magnetic dead layer thickness  $d = 1.6$  nm although the nature of magnetic state in the dead layer was not explored.<sup>7</sup>

<sup>a</sup>Corresponding author: [namottaghi@mix.wvu.edu](mailto:namottaghi@mix.wvu.edu)



It has been suggested that the “dead layer” likely contains oxygen vacancies which disrupt exchange coupling and hence destroy long range order (LRO).<sup>8</sup>

Here we report detailed magnetic studies on a 7.6 nm thick film of  $\text{La}_{0.7}\text{Sr}_{0.3}\text{MnO}_3$  on  $\text{SrTiO}_3$  (100) prepared by pulsed laser deposition (PLD). Measurements of DC magnetization ( $M$ ) were carried out in different applied magnetic fields ( $H$ ) and temperatures ( $T$ ) under the ZFC (zero-field-cooled) and FC (field-cooled) protocols to show that the blocking temperature ( $T_B$ ) usually observed in magnetic nanoparticles (NPs) is also present in thin films. In addition, isothermal hysteresis loops were measured to determine the temperature dependence of saturation magnetization ( $M_S$ ), coercivity ( $H_C$ ) and remanence ( $M_R$ ).  $M$  vs.  $T$  data show that in low  $H$ , negative remanent magnetization (NRM) exists below 100 K. Although the observation of NRM in LSMO film has been attributed to negative magnetic field trapped in superconducting magnet or uncompensated spins between ferromagnetic-ferroelectric layers,<sup>9</sup> a proper explanation for NRM is still lacking. To determine the parameters which affect the dead layer thickness  $d$ , data available from literature on the thickness ( $D$ ) variation of  $T_C$  and  $M_S$  of LSMO films grown under three different  $\text{O}_2$  pressures (200, 150 and 0.38 mTorr) are analyzed in terms of the finite size scaling, with  $M_S$  vs.  $D$  data fit to  $M_S(D) = M_S(b)(1-d/D)$  yielding the dead layer thickness  $d = 1.1, 1.4$  and  $2.4$  nm respectively ( $d = 1.4$  nm for the 7.6 nm LSMO film). Details are given below.

The LSMO thin film with  $D = 7.6$  nm was deposited on the  $\text{TiO}_2$ -terminated  $\text{SrTiO}_3$  (100) substrate from the stoichiometric  $\text{La}_{0.7}\text{Sr}_{0.3}\text{MnO}_3$  target by using a KrF excimer laser with the repetition rate of 5 Hz by PLD. During growth, the sample was heated in  $750^\circ\text{C}$  and was exposed to 100 mTorr  $\text{O}_2$  pressure and cooled down to room temperature at the rate of  $15^\circ\text{C}/\text{min}$  in 250 mTorr  $\text{O}_2$  pressure. The growth was monitored *in-situ* by reflection high energy electron diffraction (RHEED) to provide precise control of thickness down to unit cell scale. A physical property measurement system (PPMS) from Quantum Design with maximum  $H = 90$  kOe was used to measure  $M$  vs.  $T$  from 5 K to 400 K with  $H$  applied in the plane of the film. The measured magnetic moment was scaled to the volume of the film (thickness \* area). Details of the procedures for magnetic measurements are given as a note in Ref. 10.

The plots of  $M$  vs.  $T$  for the ZFC and FC cases measured in  $H = 50, 100, 200, 500$  Oe and 1 kOe are shown in Fig. 1. For the ZFC case, the sample was cooled to 5 K in  $H = 0$  Oe and measuring  $H$  was then applied and  $M$  vs.  $T$  data taken up to 400 K. For the FC case, the sample is cooled to 5 K in non-zero  $H$  and  $M$  vs.  $T$  data taken similarly up to 400 K in the cooling  $H$ . Blocking temperature  $T_B$  defined here by the bifurcation of the  $M$  (FC) from the  $M$  (ZFC) data represents the temperature above which all spins are unblocked<sup>11</sup> and  $T_B$  decreases with increasing  $H$ . As expected,  $T_B$  is less than  $T_C$ , the latter defined by the inflexion point in the  $M$  vs.  $T$  data. Note the negative magnetization for the ZFC cases below 100 K for  $H = 50$  Oe and 100 Oe. For  $H = 200$  Oe and higher  $H$ , only positive values of  $M$  (ZFC) are observed. Any negative trapped residual magnetic field was practically eliminated by demagnetizing the magnet coil as described in Ref. 10. Note that the NRM has been reported in LSMO thin films.<sup>9,12</sup> and in some nanoparticle systems also.<sup>13,14</sup>

Temperature dependence of saturation magnetization ( $M_S$ ), remanent magnetization ( $M_R$ ) and coercivity ( $H_C$ ) determined from the isothermal hysteresis loops for the ZFC sample are shown in Fig. 2. These data were corrected for the diamagnetic contribution of the substrate which was evident from the negative slope of the  $M$  vs.  $H$  plots at higher  $H$  (not shown here) where the ferromagnetic component of LSMO gets saturated. In the insets of Fig. 2, the hysteresis loop at 5 K and its low-field zoom are also shown.  $M_R$  is measured for  $H = 0$  and  $M_S$  at  $H = 4$  kOe. In Fig. 2, the initial  $M$  starts at negative values with the virgin loop requiring slightly larger field to switch sign. For  $H = 50$  Oe,  $M$  (ZFC) is negative for  $T < 100$  K becoming positive for  $T > 100$  K. In the data of  $H_C$  vs.  $T$  in Fig. 2(c),  $H_C$  has dropped below 50 Oe. This explains why for  $H < H_C$ , the  $M$  (ZFC) is negative, leading to the result that  $H < H_C$  leads to the observation of NRM for the ZFC sample.

For very thick films,  $M_S$  near 0 K was  $583$  (emu/cm<sup>3</sup>) with  $T_C \approx 350$  K.<sup>7</sup> For ferromagnetism  $M_S = N_V \mu$  where  $N_V$  is the number of spins per unit volume each with magnetic moment  $\mu$ . For  $\text{La}_{0.7}\text{Sr}_{0.3}\text{MnO}_3 = \text{La}_{0.7}^{3+}\text{Sr}_{0.3}^{2+}\text{Mn}_{0.7}^{3+}\text{Mn}_{0.3}^{4+}\text{O}_3^{2-}$  with lattice constant  $a = 0.39$  nm and calculated  $N_V = 1.68 \times 10^{22}/\text{cm}^3$  yields  $\mu = 3.74 \mu_B$  using  $M_S = 583$  emu/cm<sup>3</sup>. For  $\text{Mn}^{3+}$  ( $\text{Mn}^{4+}$ ), the expected  $\mu = 4 \mu_B$  ( $3 \mu_B$ ) using  $g = 2$ . This yields expected  $\mu/\mu_B = [(0.7)(4)+(0.3)(3)] = 3.7$  in excellent

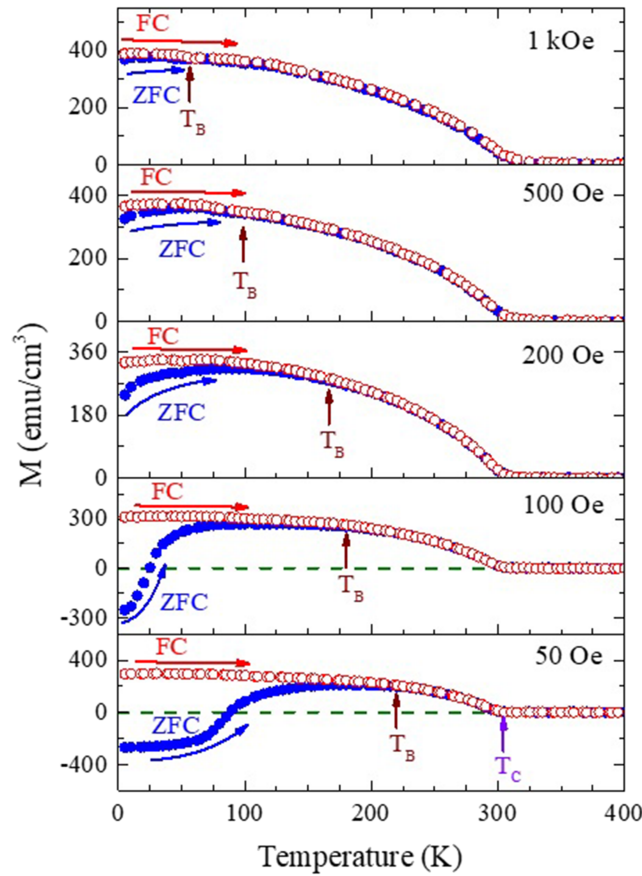


FIG. 1. Magnetization vs. temperature data for the 7.6 nm LSMO/STO sample measured with  $H = 50, 100, 200, 500$  Oe and 1 kOe. Arrows mark the bifurcation temperature  $T_B$  separating the  $M$  (FC) data (open red circles) from the  $M$  (ZFC) data (closed blue circles).  $T_C$  is the Curie temperature.

agreement with the measured  $\mu = 3.74 \mu_B$  for thick films. For the 7.6 nm thick film, the measured  $M_S = 476 \text{ (emu/cm}^3\text{)}$  is lower than  $M_S = 583 \text{ emu/cm}^3$  because of the dead layer problem discussed later. For  $M_S = 476 \text{ (emu/cm}^3\text{)}$ ,  $\mu = 3.05 \mu_B$  is obtained which gives  $S = 3/2$  for  $g = 2$  used in the calculations below.

The decrease of  $M_S$  with increasing  $T$  shown in Fig. 2(a) for the 7.6 nm film is due to the excitation of spin waves (magnons). This temperature dependence of  $M_S$  is fit to the Bloch's  $T^{3/2}$  law given by<sup>15</sup>

$$\Delta M_S / M_S(0) = (0.0597 / QS)(k_B T / 2JS)^{3/2}. \quad (1)$$

Here  $Q = 1, 2,$  or  $4$  for a sc, bcc or fcc structures and  $\Delta M_S = M_S(0) - M_S(T)$ . Bloch's law is derived using the Heisenberg Hamiltonian:  $H = -2J \sum_{i=1}^N S_i \cdot S_{i+1}$  where  $J$  is the exchange constant, and  $S_i$  is the spin of atom "i". For LSMO, there is only one magnetic ion per unit cell and so  $Q = 1$ . The lines in Fig. 2(a) are fits to Eq. (1) using  $S = 3/2$  and exchange constant  $J/k_B = 18$  K and 20 K. Thus the temperature variation of  $M_S$  can be explained by the excitation of magnons represented by the Bloch's  $T^{3/2}$  law reasonably well. Another estimate of  $J$  is determined from  $T_C$  using molecular field theory, yielding  $J/k_B = 3T_C / 2ZS(S+1)$ . With  $Z = 6$  as the number of exchange-coupled nearest neighbors each with spin  $S = 3/2$  and  $T_C = 305$  K for the 7.6 nm LSMO film gives  $J/k_B = 20$  K close to  $J/k_B = 18$  K determined above.

The temperature variation of  $M_R$  and  $H_C$  in Fig. 2 shows that both become zero near 240 K coinciding with measured  $T_B \approx 230$  K in  $H = 50$  Oe. In Fig. 3(a), the dependence of  $T_B$  on  $H$  is seen to fit very well to  $T_B(H) = T_B(0)[1 - (H/H_0)^2]$  observed in NPs.<sup>16</sup> It is proposed that the observation of a bifurcation between ZFC and FC is due to nanoclusters of spins in the dead layer of thickness

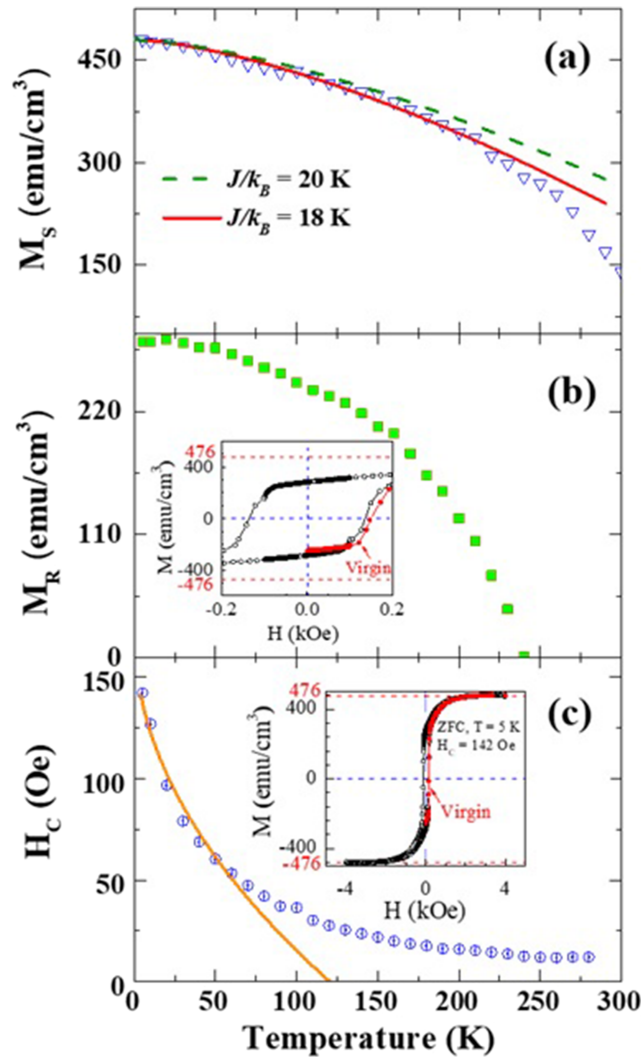


FIG. 2. Variation of  $M_S$ ,  $M_R$  and  $H_C$  vs. temperature. The solid and dashed lines in (a) are fits to Eq. (1). In the inset of (b) and (c), hysteresis loop for the low field range and up to 4 kOe respectively are shown. In (c) the solid line is fit to  $H_C(T) = H_{C0} [1 - (T/T_B)^{1/2}]$ .

$d = 1.4$  nm (determined later) in the 7.6 nm film. If  $D_0$  is the average diameter of the nanocluster, then its volume  $V \approx D_0^2 d$ . For non-interacting NPs,  $k_B T_B = KV/25$  yielding  $V = 25 k_B T_B / K$  where  $K$  is the anisotropy constant of the film.<sup>17</sup> Also the anisotropy constant  $K$  and coercivity  $H_C$  are related by the Eq.  $H_C \approx K/M_S$ . Using  $M_S = 476$  emu/cm<sup>3</sup> and  $H_C \approx 150$  Oe measured at 5K, yields  $K = 7.2 \times 10^4$  ergs/cm<sup>3</sup>. Using this value of  $K$  and  $T_B = 230$  K yields  $V = D_0^2 d = 1.1 \times 10^{-17}$  cm<sup>3</sup> leading to  $D_0 \approx 9$  nm as the diameter of the spin cluster for  $d = 1.4$  nm.

For randomly oriented and non-interacting NPs,  $H_C(T)$  vs.  $T$  varies as  $H_C(T) = H_{C0} [1 - (T/T_B)^{1/2}]$ .<sup>18,19</sup> In Fig. 2(c), the fit of the data to this Eq. for lower  $T$  appears to be valid but the fit for higher  $T$  fails and extrapolated  $T_B = 120$  K  $<$   $T_B = 230$  K with  $H = 50$  Oe. This difference is likely due to the fact that to measure  $H_C$ ,  $H = 4$  kOe was used and  $T_B$  is strongly dependent on  $H$ .

To understand the issue of the ‘dead layer’ and its role in the magnetic properties of thin films, variation of  $T_C$  and  $M_S$  with respect to film thickness  $D$  are modeled by using the available data from literature on thin films prepared in different O<sub>2</sub> deposition pressures which is shown to significantly affect the measured properties. Experiments show that  $T_C$  and  $M_S$  decrease with decrease in thickness of the films which is similar to the observations reported in magnetic NPs.<sup>6,20</sup> We model the variation of  $M_S$  vs. thickness  $D$  of thin film using the derived Eq.:  $M_S(D) = M_S(b) (1-d/D)$ ,

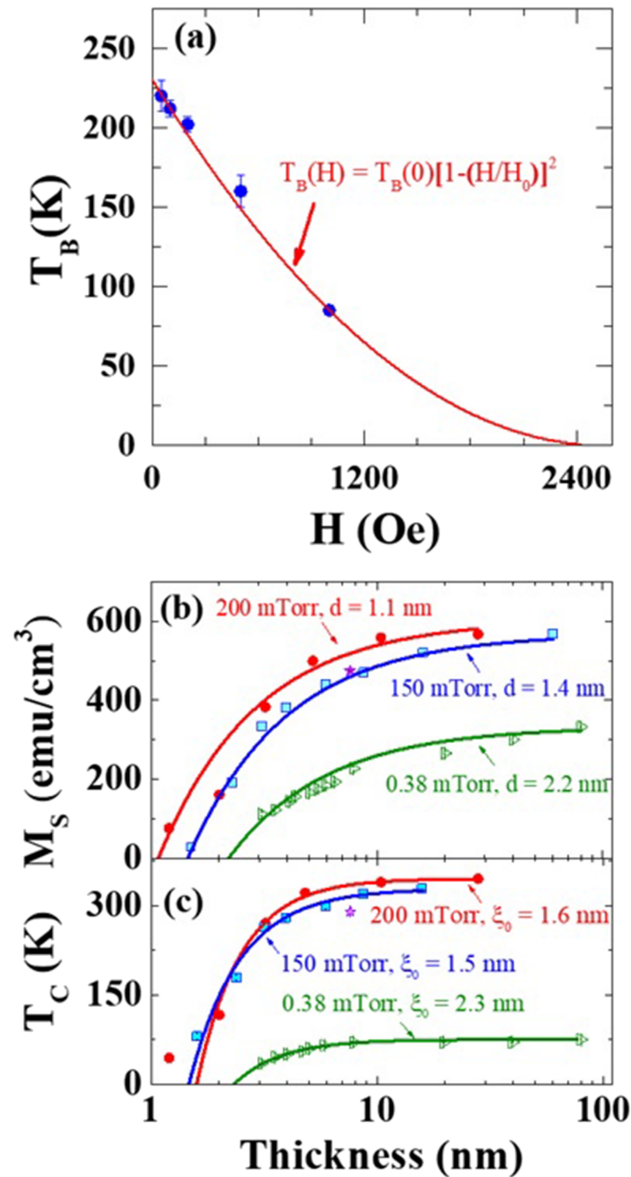


FIG. 3. (a). Variation of  $T_B$  with applied field  $H$ ; (b) Variation of the  $M_S$  and  $T_C$  with thickness  $D$  of the LSMO films. Different symbols represent data from different groups as follows: solid blue rectangle,<sup>6</sup> solid red circle,<sup>20</sup> open green diamond.<sup>7</sup> The solid lines are fits to  $M_S(d) = M_S(b)(1-d/D)$  in (b) and to Eq. (2) in (c) with the listed parameters.

where  $d$  is the thickness of dead layer which is not contributing to  $M_S$ , and  $M_S(b)$  is the saturation magnetization for bulk sample. To check the validity of this model, we show in Fig. 3(a) the plot of  $M_S$  vs.  $D$  from three sets of films grown in 200, 150 and 0.38 mTorr  $O_2$  pressures with the solid lines fits to  $M_S(D) = M_S(b)(1-d/D)$  yielding  $d = 1.1$ , 1.4 and 2.4 nm for 200, 150 and 0.38 mTorr  $O_2$  pressures respectively. For these data taken from literature,<sup>6,7,21</sup> each point was accurately determined using the internet available software ‘WebPlotDigitizer’ and the data for the 7.6 nm film is shown by the star symbol in Fig. 3. The data fit the model well, showing that with decrease in  $O_2$  pressure,  $M_S$  is lowered and  $d$  increases. Magnetic properties of manganites are governed by the double-exchange interaction between  $d$ -orbitals of magnetic  $Mn^{3+}$  and  $Mn^{4+}$  ions with charge transfer from  $Mn^{3+}$  to  $Mn^{4+}$  ions through oxygen atoms. Low  $O_2$  pressure increases oxygen vacancies, resulting in breakdown of the exchange mechanism and increased spin disorder which in turn decreases  $M_S$  and  $T_C$ .



The variation of  $T_C$  with film thickness  $D$  of LSMO films is modeled by the finite-size scaling relation:

$$T_C(D) = T_C(\infty) [1 - (\xi_0/D)^\lambda] \quad (2)$$

where  $T_C(D)$  and  $T_C(\infty)$  are respectively the Curie temperatures for a film with thickness  $D$  and very thick films,  $\lambda$  is the shift exponent and  $\xi_0$  is characteristic microscopic correlation length.<sup>22</sup> The fit of the data to Eq. (2) are shown in Fig. 3(c) for the films grown in different O<sub>2</sub> pressures with the parameters obtained from the fit listed in the figure. The value of  $\lambda$  depends on the theoretical model,  $\lambda = 2$  is obtained from Monte-Carlo simulation.<sup>23</sup>

In conclusion, using the analysis of the results from magnetic measurements, it is shown that the magnetic dead layer of thickness  $d = 1.4$  nm in the 7.6 nm LSMO film consists of clusters of ordered spins of about 9 nm diameter with nearest neighbor exchange coupling  $J/k_B \cong 18$  K among the spins. Also reported here is the observation of NRM in ZFC samples with measuring  $H < H_C$ . Additional studies on the origin of NRM are in progress and these results will be reported soon.

We acknowledge funding support from NSF (DMR-1608656) for the growth, optimization and characterization of films and DOE (DE-SC0016176) for the theoretical discussion and fits.

- <sup>1</sup> N. Izyumskaya, Y. Alivov, and H. Morkoc, *Crit. Rev. Solid State Mater. Sci.* **34**, 89 (2009).
- <sup>2</sup> A. Urushibara, Y. Moritomo, T. Arima, A. Asamitsu, G. Kido, and Y. Tokura, *Phys. Rev. B* **51**, 14103 (1995).
- <sup>3</sup> C. Moreno, C. Munuera, S. Valencia, F. Kronast, X. Obradors, and C. Ocal, *Nano Lett.* **10**, 3828 (2010).
- <sup>4</sup> L. You, C. Lu, P. Yang, G. Han, T. Wu, U. Luders, W. Prellier, K. Yao, L. Chen, and J. Wang, *Adv. Mater.* **22**, 4964 (2010).
- <sup>5</sup> R. Martínez, A. Kumar, R. Palai, J. Scott, and R. Katiyar, *J. Phys. Appl. Phys.* **44**, 105302 (2011).
- <sup>6</sup> M. Huijben, L. Martin, Y.-H. Chu, M. Holcomb, P. Yu, G. Rijnders, D. H. Blank, and R. Ramesh, *Phys. Rev. B* **78**, 094413 (2008).
- <sup>7</sup> Å. Monsen, J. E. Boschker, F. Macià, J. W. Wells, P. Nordblad, A. D. Kent, R. Mathieu, T. Tybell, and E. Wahlström, *J. Magn. Magn. Mater.* **369**, 197 (2014).
- <sup>8</sup> R. Peng, H. C. Xu, M. Xia, J. F. Zhao, X. Xie, D. F. Xu, B. P. Xie, and D. L. Feng, *Appl. Phys. Lett.* **104**, 081606 (2014).
- <sup>9</sup> S. Dussan, A. Kumar, J. Scott, S. Priya, and R. Katiyar, *Appl. Phys. Lett.* **97**, 252902 (2010).
- <sup>10</sup> For each measurement, the magnet coil was first demagnetized at ambient since without demagnetizing the coil, the residual  $H \sim 25$  Oe is present but after demagnetizing the coil, the residual  $H$  is reduced to  $< 2$  Oe. Next the sample centering was done at ambient in  $H = 1$  kOe, followed by raising the temperature to 360 K (which is above  $T_C$ ) to remove any remanence in the sample. The sample was then cooled to 5 K in zero applied  $H$ . After waiting for 15 minutes at 5 K to ensure temperature stability, a measuring  $H$  was then applied. For measuring  $M$  vs.  $T$  starting from 5 K, a sequence file is created for the temperatures at which  $M$  is to be measured, typically in 2-degree steps. The temperature sweep rate was 5 K/min but temperature is stabilized at each measuring temperature for about 15 seconds during which the data of magnetic moment at that temperature is acquired. The system then automatically goes to the next measuring temperature and the procedure is repeated. The isothermal data of  $M$  vs.  $H$  were acquired using similar procedures. The lateral dimensions of the film and substrate are: 4.98 mm  $\times$  5.81 mm.
- <sup>11</sup> K. L. Pisane, E. C. Despeaux, and M. S. Seehra, *J. Magn. Magn. Mater.* **384**, 148 (2015).
- <sup>12</sup> J.-S. Lee, D. Arena, P. Yu, C. Nelson, R. Fan, C. Kinane, S. Langridge, M. Rossell, R. Ramesh, and C.-C. Kao, *Phys. Rev. Lett.* **105**, 257204 (2010).
- <sup>13</sup> N. Menyuk, K. Dwight, and D. Wickham, *Phys. Rev. Lett.* **4**, 119 (1960).
- <sup>14</sup> A. Kumar and S. Yusuf, *Phys. Rep.* **556**, 1 (2015).
- <sup>15</sup> F. Holtzberg, T. McGuire, S. Methfessel, and J. Suits, *J. Appl. Phys.* **35**, 1033 (1964).
- <sup>16</sup> V. Singh, M. S. Seehra, and J. Bonevich, *J. Appl. Phys.* **103**, 07D524 (2008).
- <sup>17</sup> P. Dutta, S. Pal, M. Seehra, M. Anand, and C. Roberts, *Appl. Phys. Lett.* **90**, 213102 (2007).
- <sup>18</sup> F. Fonseca, G. Goya, R. Jardim, R. Muccillo, N. Carreno, E. Longo, and E. Leite, *Phys. Rev. B* **66**, 104406 (2002).
- <sup>19</sup> D. Peng, T. Hihara, K. Sumiyama, and H. Morikawa, *J. Appl. Phys.* **92**, 3075 (2002).
- <sup>20</sup> S. Roy, I. Dubenko, D. D. Edorh, and N. Ali, *J. Appl. Phys.* **96**, 1202 (2004).
- <sup>21</sup> C. Wang, K. Jin, L. Gu, H. Lu, S. Li, W. Zhou, R. Zhao, H. Guo, M. He, and G. Yang, *Appl. Phys. Lett.* **102**, 252401 (2013).
- <sup>22</sup> S. Thota, J. Shim, and M. Seehra, *J. Appl. Phys.* **114**, 214307 (2013).
- <sup>23</sup> O. Iglesias and A. Labarta, *Phys. Rev. B* **63**, 184416 (2001).